Three-Layer Perceptron versus Radial Basis Function for the Low-pass Equivalent Behavioral Modeling of Wireless Transmitters

Caroline de França, Luiza Beana Chipansky Freire and Eduardo Gonçalves de Lima
Electrical Engineering Department, Federal University of Paraná, Curitiba, PR 81531-980, Brazil
(caroldf90@hotmail.com, luiza.chipans@gmail.com, elima@eletrica.ufpr.br)

***Abstract*— This paper addresses the low-pass equivalent behavioral modeling of wireless transmitters using artificial neural networks (ANNs). Radial basis function (RBF) and three-layer perceptron (TLP) are the most widely adopted ANN architectures. In wireless transmitter behavioral modeling literature, it is reported the effective use of either TLP or RBF. The contribution of this work is to present a comparative study between TLP and RBF in terms of computational complexity and modeling accuracy. In here, the basic requirements that the ANN-based models must comply with to properly model the behavior of bandpass systems is first identified. Then, both TLP and RBF are applied to the low-pass equivalent behavioral modeling of three different wireless transmitters: a GaN HEMT class AB, a Si LDMOS class AB and a GaN HEMT Doherty. For the three studied transmitters, RBF models trained by the orthogonal least squares algorithm do not provide acceptable modeling accuracies, while TLP models trained by the back-propagation algorithm do produce highly accurate models. For a fair comparison between TLP and RBF models, all models are then trained by the same nonlinear optimization tool based on the Gauss-Newton algorithm with line search. Indeed, by changing the training algorithm, the modeling accuracy of RBF models is significantly improved for the three studied transmitters. In the one hand, for the GaN HEMT Doherty transmitter in a scenario of similar number of network parameters, it is verified that the TLP provides a significant higher accuracy than the RBF, illustrated by improvements in NMSE and ACEPR metrics by up to 8.4 dB and 8.7 dB, respectively. On the other hand, for the GaN HEMT class AB and Si LDMOS class AB transmitters in a scenario of similar number of network parameters, the TLP and RBF modeling accuracies are very similar, although a slight superior performance is observed for TLP models, quantified by up to 0.7 dB and 1.5 dB improvements in NMSE and ACEPR metrics, respectively.**

***Index Terms*—** Bandpass systems, digital baseband predistortion, modeling, radial basis function, three layer perceptron, wireless communication systems.

I. INTRODUCTION

Standards for modern wireless communication systems target the communication of an enormous amount of information, at extremely high data rates and through a very narrowband air interface, at the same time obeying severe requirements on quality-of-service (QoS) [1]. The very high data rates

Brazilian Microwave and Optoelectronics Society-SBMO *received 27 Feb 2015; for review 01 Mar 2015; accepted 19 Sep 2015*
Brazilian Society of Electromagnetism-SBMag *ISSN 2179-1074*

promised by modern wireless standards have motivated the rapid growth and widespread use of internet services through the cellular networks. The successful achievement of the standard goals is strongly conditioned by the linear transmission of a radio frequency (RF) carrier signal modulated by envelope signals having a high peak to average power ratio (PAPR). Nevertheless, the demand for linearity in the transmission of envelope signals having a high PAPR critically affects the power efficiency [2], [3].

Power efficiency has always been an important subject in wireless communication systems [4]. In base-stations, the power levels that must be handled are very high and, therefore, increasing power efficiency is a fundamental objective, directly related to the costs associated with heat dissipation and energy consumption. Besides, in battery-driven handsets, improving the power efficiency is highly desired, especially for achieving longer time of battery autonomy. The RF power amplifier (PA) present in the wireless transmitter chain plays a major role in determining the overall power efficiency of a wireless communication system. In fact, RF PA efficiency is strongly affected by two fundamental behaviors observed in solid state power transistors, independent of their class of operation [5]. First, power transistors can only provide a high efficiency at a single power level. Second, power transistors exhibit an intrinsically trade-off between linearity and efficiency. In other words, a PA provides the highest efficiency when driven at strong compression level where its nonlinear behavior can not be neglected. Moreover, as the input power level is reduced to improve the linearity, the PA efficiency reduces as well.

To comply with the rigorous requirements on linearity imposed by modern wireless standards, the PA must be driven at very low power levels to guarantee a linear amplification of the envelope peak level. As a consequence, the PA average output power must be substantially reduced from its saturation power level, which results in poor power efficiency. The simultaneous demands for linearity and efficiency can only be achieved if a linearization scheme is included in the transmitter chain. Digital baseband predistortion (DPD) is a common adopted linearization solution [6]. A crucial step to the design of an effective DPD scheme is the selection of a high accurate and low complexity nonlinear dynamic model for the wireless transmitter [7].

Artificial neural networks (ANNs) can be employed as the required wireless transmitter model for DPD purposes [8]. Two architectures of ANNs are most widely reported in literature, namely the three-layer perceptron (TLP) and the radial basis function (RBF) [8]. Specifically for the low-pass equivalent behavioral modeling of RF PAs, [9]-[13] reported the application of TLP, while in [14] and [15] it is documented the application of RBF. However, [9]-[15] have not compared TLP and RBF. The contribution of this work is to present a careful comparison between TLP- and RBF-based behavioral models, paying attention to guarantee that all models satisfy the fundamental constraints imposed by the bandpass behavior of wireless transmitters under narrowband excitations and focusing on the investigation of the modeling accuracy as a function of the computational cost, estimated by the number of network parameters.

Brazilian Microwave and Optoelectronics Society-SBMO *received 27 Feb 2015; for review 01 Mar 2015; accepted 19 Sep 2015*
Brazilian Society of Electromagnetism-SBMag *ISSN 2179-1074*

This work is organized as follows. Section II reviews the TLP and RBF architectures. Section III describes the impact of the bandpass behavior of wireless transmitters on ANN-based low-pass equivalent behavioral models. Section IV comparatively assesses the computational cost and modeling accuracy of TLP- and RBF-based behavioral models, based on input-output data obtained from three different wireless transmitters. Finally, conclusions are summarized in Section V.

II. ARTIFICIAL NEURAL NETWORKS

Feed-forward ANNs are widely used in communication systems for the modeling of dynamic nonlinear systems. In comparison with polynomial-based approximations, ANNs require a lower number of parameters and behave better outside the training subspace. Three-layer perceptron (TLP) and radial basis function (RBF) are the most widely reported architectures for feed-forward ANNs. Figure 1(a) shows the block diagram of a TLP, while the block diagram of an RBF is shown in Fig. 1(b). Observe that the ANNs shown in Fig. 1 have *E* inputs, *R* neurons in the hidden layer and *S* outputs.

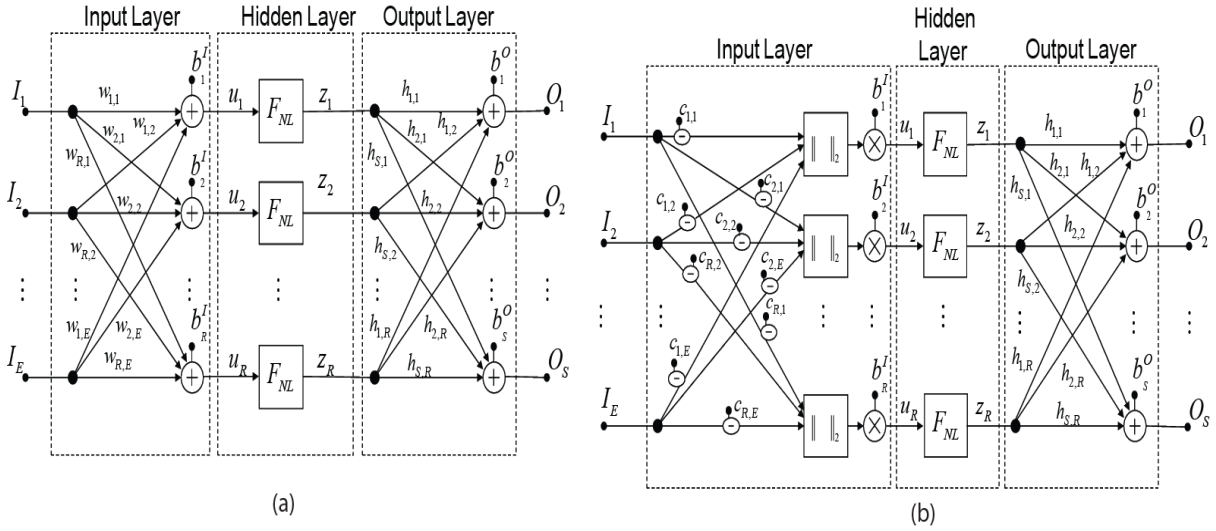

Fig. 1. Block diagram of feed-forward ANNs: (a) three-layer perceptron (TLP) and (b) radial basis function (RBF).

In a TLP, the *E* input signals are first multiplied by input weights (w) and added to input biases (b^I), then applied to activation functions (F_{NL}) and, finally, multiplied by output weights (h) and added to output biases (b^O). Nonlinear activation functions are required when the TLP is used to model nonlinear systems. The hyperbolic tangent sigmoid function

$$F_{NL}(u) = \frac{2}{1+\exp(-2u)} - 1 \tag{1}$$

can provide the adequate TLP activation function. The TLP network parameters (w, b^I, h, b^O) are usually identified by the back-propagation (BP) algorithm [8]. Starting from an initial guess for all the TLP network parameters, the BP algorithm is an iterative procedure that performs two steps at each iteration. In the first (or forward) step, the TLP input signals are propagated throughout the TLP to calculate the error signal defined by the difference between desired and estimated outputs. In the second step, the error signal is back propagated throughout the TLP in order to update the values of all

Brazilian Microwave and Optoelectronics Society-SBMO *received 27 Feb 2015; for review 01 Mar 2015; accepted 19 Sep 2015*
Brazilian Society of Electromagnetism-SBMag *ISSN 2179-1074*

the TLP network parameters.

In an RBF, the input signals are treated as a vector of dimension *E*. For each one of the *R* neurons in the hidden layer, a vector (also of dimension *E*) called center vector is defined, having as coefficients the RBF parameters *c*. The signals *u* applied to the activation functions (F_{NL}) are obtained by first taking the Euclidean distance between the input vector and the neuron center vector and then multiplying the obtained results by input bias (b^I) parameters. The Gaussian function

$$F_{NL}(u) = \exp(-u^2), \tag{2}$$

can provide the required RBF activation function. The *O* output signals are given by the linear combination of the signals *z* at the output of the activation functions, weighted by the output parameters (*h*) and added to output biases (b^O). The RBF network parameters are commonly extracted by the orthogonal least squares algorithm [16]. The RBF is a nonlinear function of its network parameters. However, if the center parameters (*c*) are available, then the RBF is a linear function of the weight and output bias parameters (*h* and b^O). The strategy followed in [16] is to divide the training algorithm into two steps. In the first step, the centers are chosen in a non optimal way. In fact, the centers are constrained to be exactly equal to the values applied as inputs at a particular time instant. The numerical values applied as inputs at each time instant are potential candidates for the centers. A search among all the potential candidates is then executed to identify the best choices for the centers. In the second step, a linear identification algorithm is performed to obtain the weight and output bias parameters. Instead of using the least squares (LS) to perform this task, in [16] it is employed the orthogonal least squares (OLS). Indeed, the OLS is less susceptible to be ill-conditioned than the LS because the regression matrix that must be inverted during the training is orthogonal in the OLS. Besides, in the OLS the parameters *h* and b^O can be identified one by one, once the training for each parameter is completely independent from the training for the other parameters. Therefore, by using the OLS the search executed in the step one is simplified, because now it is possible to replace a single large search with *R* smaller searches, where *R* indicates the number of neurons in the hidden layer.

Considering that the TLP and RBF standard training algorithms (namely the BP and OLS algorithms, respectively) are very distinct from each other, to provide a fair comparison in this work TLP and RBF models are also trained by the nonlinear optimization tool based on the Gauss-Newton algorithm with line search described in [17].

III. ANN-BASED LOW-PASS EQUIVALENT BEHAVIORAL MODELING OF WIRELESS TRANSMITTERS

Bandpass signals are defined as signals having a bandwidth much lower than the center frequency. Wireless transmitters are systems having one input and one output, which relate bandpass signals. Denoting the bandpass input and output signals by *x* and *y*, respectively, and assuming a center frequency equal to the RF carrier frequency ω_c, the complex-valued input $\tilde{x}$ and output $\tilde{y}$ envelopes are obtained from:

Brazilian Microwave and Optoelectronics Society-SBMO *received 27 Feb 2015; for review 01 Mar 2015; accepted 19 Sep 2015*
Brazilian Society of Electromagnetism-SBMag *ISSN 2179-1074*

$$x = \mathrm{Re}\left[\tilde{x} e^{j\omega_c t} \right] = a\cos\left(\omega_c t + \theta\right), \tag{3}$$

and

$$y = \mathrm{Re}\left[\tilde{y} e^{j\omega_c t} \right] = b\cos\left(\omega_c t + \varphi + \theta\right). \tag{4}$$

An accurate discrete-time wireless transmitter model that estimates *y* as a function of *x* requires a huge computational cost, which is unacceptable for linearization applications. The reasoning is as follows. First, to satisfy the Nyquist criterion, the sampling frequency of a model relating bandpass signals must be at least twice the carrier frequency (on the order of GHz). Second, the wireless transmitter model must estimate low-frequency memory effects (on the order of MHz) due to transistor self-heating and biasing-circuitry. Therefore, to simultaneously comply with these two requirements, the instantaneous wireless transmitter output must be formulated as a function of the instantaneous, as well as an extremely large set (on the order of thousands) of previous, wireless transmitter inputs.

Behavioral models having a much lower computational cost, and so suitable for DPD purposes, can be obtained by exploiting the fact that bandpass signals have non-null energy only at frequencies near ω_c. The basic idea is to describe the complex-valued output envelope $\tilde{y}$ as a function of only the complex-valued input envelope $\tilde{x}$, e.g. $\tilde{y} = f(\tilde{x})$. In doing that, the maximum frequency that the model must handle is reduced to a few times the envelope bandwidth. Hence, a sampling frequency on the MHz range is enough to fulfill the Nyquist criterion. Therefore, the instantaneous wireless transmitter output can be accurately modeled by a function of a few variables, including the instantaneous plus a few previous samples of the wireless transmitter input. These compact models are known in literature as low-pass equivalent behavioral models. Once the particular value of ω_c have no effect on the low-pass equivalent behavioral models, if $\tilde{x}$ is subject to an arbitrary nonlinear operator *f*, contributions having non-null energy also at harmonic frequencies of ω_c can easily be generated, even though they can not be attributed to any measurement performed on the wireless transmitter.

In order to guarantee that only physical in-band responses are generated by the low-pass equivalent behavioral models, the operator *f* must comply with some bandpass constraints. As shown in [10], the operator *f* must be chosen in a way that the unitary scalar value multiplying the carrier frequency ω_c is preserved, e.g. the expression $1\omega_c t$ must be retained. The use of a model that satisfies the bandpass constraints is strongly recommended. In fact, the computational complexity of a low-pass equivalent behavioral model can be significantly reduced, if it is avoided the generation of out-of-band contributions that have no physical counterpart and, therefore, can not contribute to improve the modeling accuracy.

Now, attention is turned to adapt the ANNs described in Section II, in order to apply them to the behavioral modeling of bandpass systems, in a way that only physical in-band contributions are generated. It is worth mentioning that, in here, the ANN inputs, outputs, weights and biases are

Brazilian Microwave and Optoelectronics Society-SBMO *received 27 Feb 2015; for review 01 Mar 2015; accepted 19 Sep 2015*
Brazilian Society of Electromagnetism-SBMag *ISSN 2179-1074*

restricted to real-valued numbers. Following the strategy proposed in [13], in this work the ANNs, of TLP or RBF architectures, have as inputs and outputs the signals shown in Fig. 2. First, observe that the amplitude (or absolute value) of an envelope signal has no relation with the carrier frequency. Second, note that the polar angle of an envelope signal (θ) is intrinsically connected to ω_c by the expression $(\omega_C t + \theta)$. However, by taking the difference between any two arbitrary polar angles, for instance $(\omega_C t + \theta_1) - (\omega_C t + \theta_2) = (\theta_1 - \theta_2)$, it is possible to separate the argument θ from ω_c. Therefore, if only baseband signals, keeping no information about ω_c, are applied as inputs to an ANN, the estimated signal at the ANN output is also restricted to a baseband signal. In other words, it is impossible to generate integer multiples of ω_c. Furthermore, observe that additional operations must be performed over the output of the ANNs to restore the unitary scalar value multiplying the carrier frequency ω_c, as shown in Fig. 2. Moreover, to account for memory effects, the ANN has as inputs the instantaneous (*n*) as well as past samples (*n-M*) up to the memory length *M*.

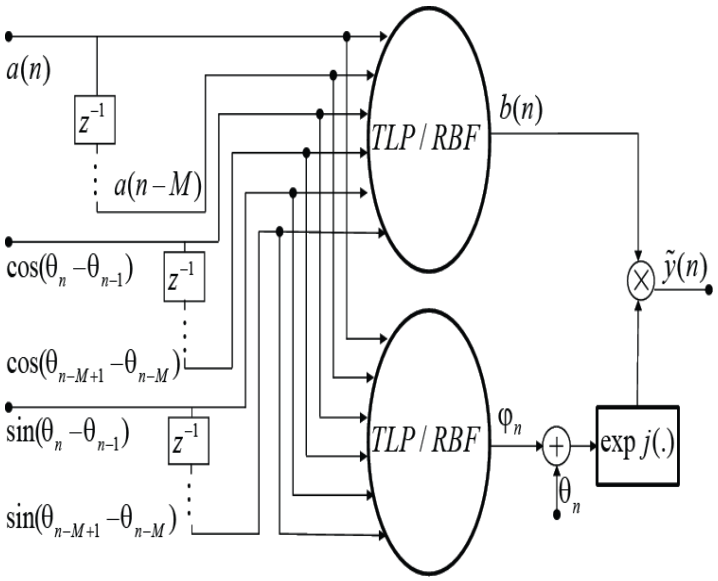

Fig. 2. Block diagram of ANN-based low-pass equivalent wireless transmitter behavioral models [13].

IV. COMPARATIVE ANALYSIS BETWEEN TLP AND RBF

In this section, a careful comparison between TLP and RBF, when applied to the behavioral modeling of wireless transmitters, is performed. Two realizations of the block diagram shown in Fig. 2 are implemented in Matlab software, differentiated to each other only by the used ANN: TLP in one case and RFB in the other case. The TLP has hyperbolic tangent sigmoid activation functions, given by (1), and is trained by the back-propagation (BP) algorithm [8] and the Gauss-Newton (GN) algorithm with line search [17], while the RBF has Gaussian activation functions, according to (2), and is trained by the orthogonal least squares (OLS) algorithm [16] and the Gauss-Newton (GN) algorithm with line search [17].

Three different devices-under-test (DUTs) are investigated. In all cases, the input-output data was divided into two subsets: one for the network training and one for the network validation. Only validation results are reported here. The model accuracy is measured by two metrics performed on

Brazilian Microwave and Optoelectronics Society-SBMO received 27 Feb 2015; for review 01 Mar 2015; accepted 19 Sep 2015
Brazilian Society of Electromagnetism-SBMag *ISSN 2179-1074*

error signals defined by the difference between estimated and desired wireless transmitter outputs: the normalized mean-square error (NMSE), as defined in [18], and the adjacent channel error power ratio (ACEPR), as defined in [19].

A. GaN HEMT class AB power amplifier

The first studied DUT is a GaN HEMT class AB power amplifier (PA), excited by a carrier frequency of 900 MHz modulated by a two-carrier 3GPP WCDMA signal, each carrier having a bandwidth of 3.84 MHz and shifted by 5 MHz. The input-output data was measured with a Rohde & Schwarz FSQ vector signal analyzer (VSA) at a sampling frequency of 61.44 MHz, when the RF PA was operated at an average output power equal to 26 dBm.

Two different investigations are performed. In the first investigation, several particular instances of TLP and RBF models, having a variable number of neurons in the hidden layer but a fixed memory length $M = 2$, are implemented in Matlab software. Figure 3 shows the best ACEPR and NMSE results as a function of the number of network parameters for TLP models, while Fig. 4 shows the best ACEPR and NMSE results as a function of the number of network parameters for RBF models. Observe from Fig. 3 that the choice of the TLP training algorithm has a little effect on the modeling accuracy. Specifically, in case of same number of network parameters, the largest difference between TLP models trained by BP and GN algorithms is quantified by 0.8 dB in NMSE and 2.0 dB in ACEPR. However, from Fig. 4, observe that the choice of the RBF training algorithm has a very significant effect on the modeling accuracy. For instance, in case of same number of network parameters, the largest difference between RBF models trained by OLS and GN algorithms is quantified by 23.3 dB in NMSE and 21.5 dB in ACEPR. More important, RBF models trained by the OLS algorithm do not provide acceptable levels of modeling accuracy.

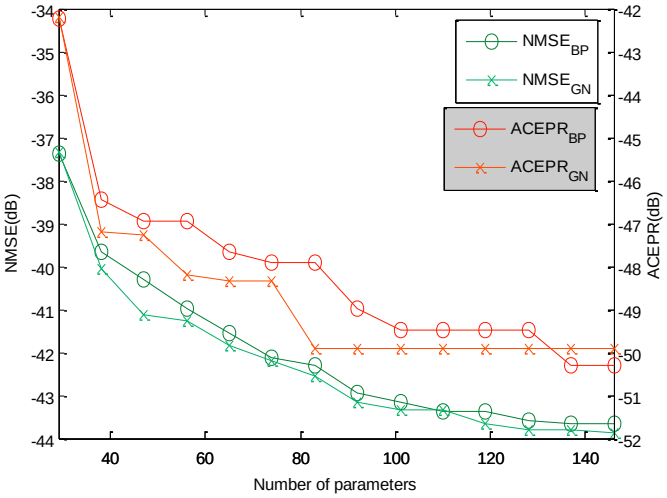

Fig. 3. NMSE and ACEPR (largest from lower and upper adjacent channels, bandwidth of 3.84 MHz for main and adjacent channels, frequency shift of 5 MHz between main and adjacent channels) for TLP models and GaN HEMT class AB.

ISSN 2179-1074

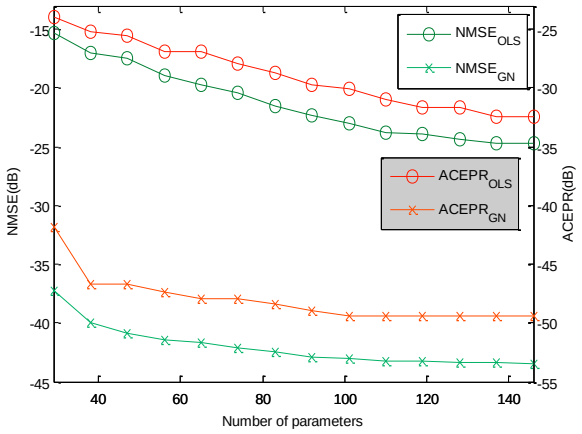

Fig. 4. NMSE and ACEPR (largest from lower and upper adjacent channels, bandwidth of 3.84 MHz for main and adjacent channels, frequency shift of 5 MHz between main and adjacent channels) results for RBF models and GaN HEMT class AB.

In the second investigation, the accuracies of TLP and RBF models are compared for the case in which they are both trained by the GN algorithm. Several particular instances of TLP and RBF models, having a variable number of neurons in the hidden layer and a variable memory length *M*, are implemented in Matlab software. Figure 5 shows the best ACEPR and NMSE results as a function of the number of network parameters. Notice from Fig. 5 that the TLP and RBF models provide very similar trade-offs between modeling error and computational cost. In particular, TLP models show a slight superior performance than RBF models, achieving higher accuracies (up to 0.5 dB and 1.5 dB improvements in NMSE and ACEPR results, respectively) in case of same number of parameters.

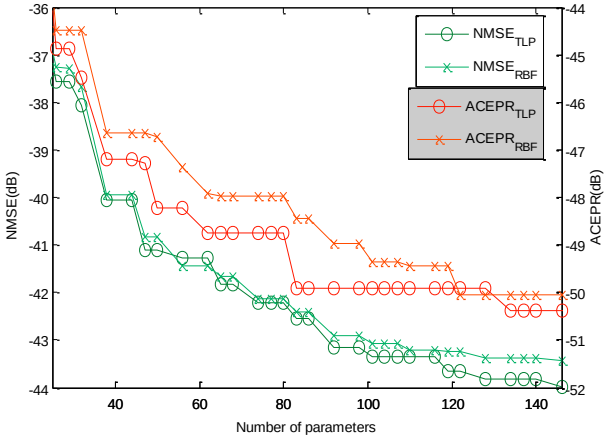

Fig. 5. NMSE and ACEPR (largest from lower and upper adjacent channels, bandwidth of 3.84 MHz for main and adjacent channels, frequency shift of 5 MHz between main and adjacent channels) results for GaN HEMT class AB.

The modeling accuracies of TLP and RBF models are further illustrated by the power spectral densities (PSDs) shown in Fig. 6. A sequence of 4096 time-domain samples is first applied to a Blackman window [20] and then mapped to the frequency-domain using a fast Fourier transform (FFT) algorithm. To provide a clear picture of the spectral content, the frequency-domain samples are divided into 128 groups, each group containing 32 consecutive frequency-domain samples. The average values of each group are calculated. Only the 128 average values are plotted in Fig. 6.

Brazilian Microwave and Optoelectronics Society-SBMO *received 27 Feb 2015; for review 01 Mar 2015; accepted 19 Sep 2015*
Brazilian Society of Electromagnetism-SBMag *ISSN 2179-1074*

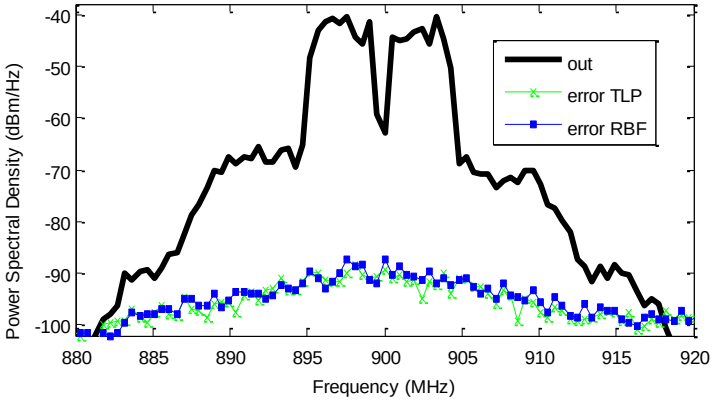

Fig. 6. PSD of the error signals for TLP and RBF models having 146 network parameters, when modeling the GaN HEMT class AB.

The TLP model reported in Fig. 6 has 146 parameters and provides the excellent NMSE and ACEPR results of -44.0 dB and -50.4 dB, respectively. The RBF model reported in Fig. 6 also has 146 parameters and provides the very good NMSE and ACEPR results of -43.4 dB and -50.1 dB, respectively. From Fig. 6, when the TLP model is used instead of the RBF model having an equal number of parameters, a slight reduction in the PSD of the error signal is observed in mostly of the displayed spectral range.

B. Si LDMOS class AB power amplifier

The second investigated DUT is a Si LDMOS class AB PA, excited by a carrier frequency of 2 GHz modulated by a 3GPP WCDMA envelope signal having a bandwidth of 3.84 MHz. The input-output data was measured with an Agilent MXA N9020A VSA at a sampling frequency of 30.72 MHz, when the RF PA was operated at an average output power equal to 31.5 dBm. Again, two different analyses are performed. In the first analysis, several TLP and RBF models, having a variable number of neurons in the hidden layer but a fixed memory length $M = 1$, are implemented in Matlab software. Figure 7 shows the best ACEPR and NMSE results as a function of the number of network parameters for TLP models, while Fig. 8 shows the best ACEPR and NMSE results as a function of the number of network parameters for RBF models. Observe from Fig. 7 that, again, the choice of the TLP training algorithm has a little effect on the modeling accuracy. Specifically, in case of same number of network parameters, the largest difference between TLP models trained by BP and GN algorithms is quantified by 0.1 dB in NMSE and 0.6 dB in ACEPR. However, from Fig. 8, observe that the choice of the RBF training algorithm has a very significant effect on the modeling accuracy. Specifically, in case of same number of network parameters, the largest difference between RBF models trained by OLS and GN algorithms is quantified by 12.1 dB in NMSE and 18.2 dB in ACEPR. Hence, RBF models trained by the OLS algorithm do not provide acceptable levels of modeling accuracy also for the second investigated DUT.

Brazilian Microwave and Optoelectronics Society-SBMO *received 27 Feb 2015; for review 01 Mar 2015; accepted 19 Sep 2015*
Brazilian Society of Electromagnetism-SBMag *ISSN 2179-1074*

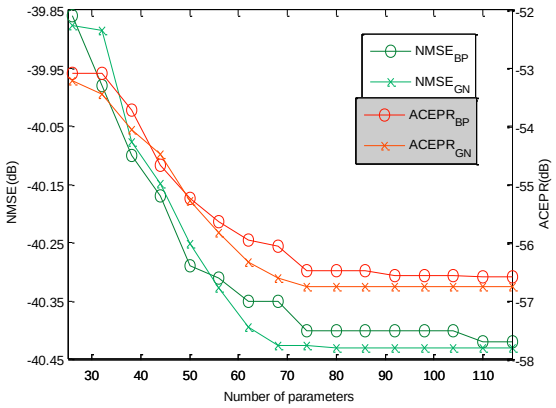

Fig. 7. NMSE and ACEPR (largest from lower and upper adjacent channels, bandwidth of 3.84 MHz for main and adjacent channels, frequency shift of 5 MHz between main and adjacent channels) results for TLP models and Si LDMOS class AB.

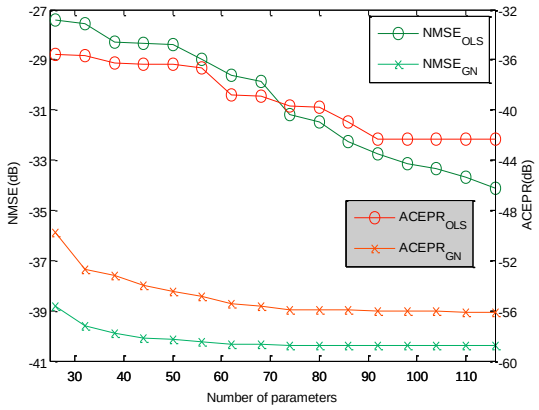

Fig. 8. NMSE and ACEPR (largest from lower and upper adjacent channels, bandwidth of 3.84 MHz for main and adjacent channels, frequency shift of 5 MHz between main and adjacent channels) results for RBF models and Si LDMOS class AB.

In the second analysis, the accuracies of TLP and RBF models are compared for the case in which they are both trained by the GN algorithm. Several TLP and RBF models, having a variable number of neurons in the hidden layer and a variable memory length *M*, are implemented in Matlab software. Figure 9 shows the best ACEPR and NMSE results as a function of the number of network parameters. Notice from Fig. 9 that, once more, TLP and RBF models provide very similar trade-offs between modeling error and computational cost. Indeed, in a scenario of equal number of parameters, Fig. 9 shows that TLP models provide a little better accuracy than RBF models, quantified by up to 0.7 dB and 1.2 dB improvements in NMSE and ACEPR metrics, respectively.

Additionally, the PSDs of the error signals shown in Fig. 10 also confirm that the modeling fidelity achieved by TLP and RBF models having an equal number of parameters is very similar. The same procedure adopted in Fig. 6 is also applied to generate the PSD plots shown in Fig. 10 and, hence, only 128 average values (from a total of 4096 samples) are plotted in Fig. 10.

The TLP model reported in Fig. 10 has 98 parameters and provides the excellent NMSE and ACEPR results of -41.1 dB and -57.2 dB, respectively. The RBF model reported in Fig. 10 also has 98 parameters and provides the very good NMSE and ACEPR results of -40.4 dB and -56.1 dB, respectively. From Fig. 10, when the TLP model is used instead of the RBF model having an equal

  ISSN 2179-1074

number of parameters, a small reduction in the PSD of the error signal is observed, especially inside the signal channel and at the lower adjacent channel.

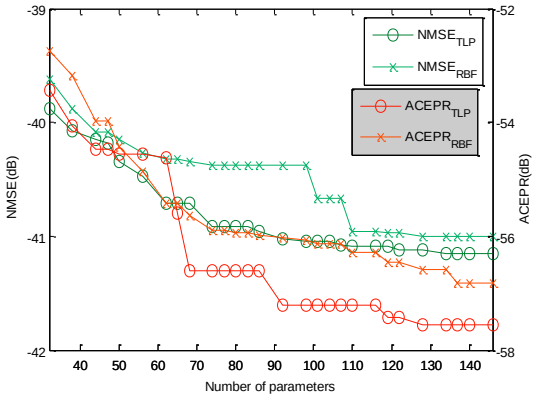

Fig. 9. NMSE and ACEPR (largest from lower and upper adjacent channels, bandwidth of 3.84 MHz for main and adjacent channels, frequency shift of 5 MHz between main and adjacent channels) results for Si LDMOS class AB.

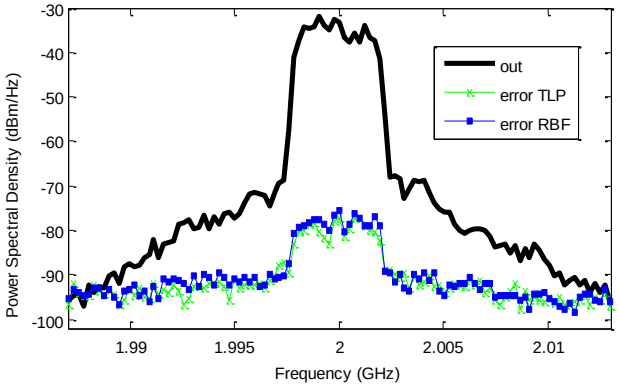

Fig. 10. PSD of the error signals for TLP and RBF models having 98 network parameters, when modeling the Si LDMOS class AB.

C. GaN HEMT Doherty power amplifier

The third analyzed DUT is a GaN HEMT Doherty PA, excited by a carrier frequency of 2.14 GHz modulated by a LTE OFDMA envelope signal having a bandwidth of 10 MHz. The input-output data was obtained from a circuit simulator, when the RF PA was operated at an average output power equal to 30.5 dBm.

Once more, two different investigations are performed. In the first investigation, different TLP and RBF models, having a variable number of neurons in the hidden layer but a fixed memory length M = 1, are implemented in Matlab software. Figure 11 shows the best ACEPR and NMSE results as a function of the number of network parameters for TLP models, while Fig. 12 shows the best ACEPR and NMSE results as a function of the number of network parameters for RBF models. From Fig. 11, as was the case with the two previously assessed DUTs, observe that the choice of the TLP training algorithm has a little effect on the modeling accuracy. Specifically, in case of same number of network parameters, the largest difference between TLP models trained by BP and GN algorithms is quantified by 0.9 dB in NMSE and 1.6 dB in ACEPR. However, from Fig. 12 observe that the choice of the RBF training algorithm has a very important effect on the modeling accuracy. Specifically, in

Brazilian Microwave and Optoelectronics Society-SBMO *received 27 Feb 2015; for review 01 Mar 2015; accepted 19 Sep 2015*
Brazilian Society of Electromagnetism-SBMag *ISSN 2179-1074*

case of same number of network parameters, the largest difference between RBF models trained by OLS and GN algorithms is quantified by 11.1 dB in NMSE and 10.5 dB in ACEPR. Therefore, RBF models trained by the OLS algorithm do not provide acceptable levels of modeling accuracy for anyone of the three studied DUTs.

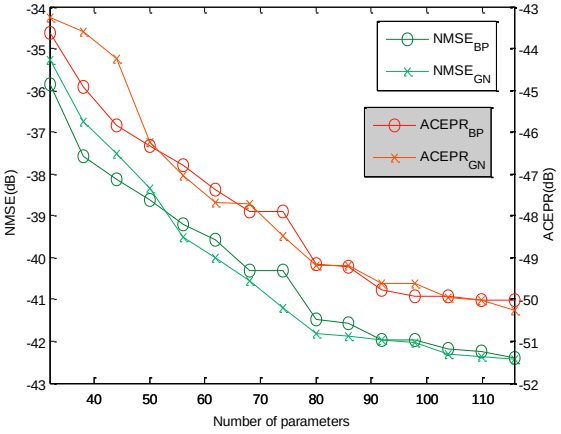

Fig. 11. NMSE and ACEPR (largest from lower and upper adjacent channels, bandwidth of 7.68 MHz for main and adjacent channels, frequency shift of 10 MHz between main and adjacent channels) results for TLP models and GaN HEMT Doherty.

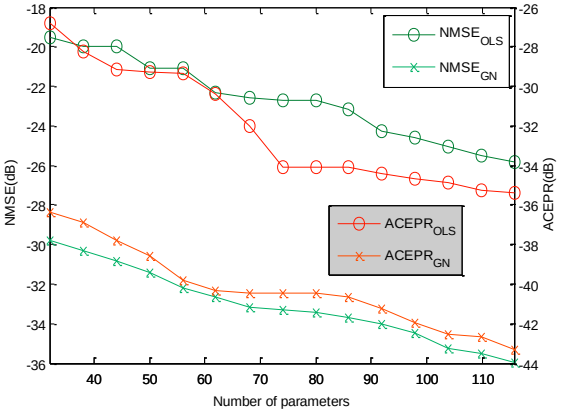

Fig. 12. NMSE and ACEPR (largest from lower and upper adjacent channels, bandwidth of 7.68 MHz for main and adjacent channels, frequency shift of 10 MHz between main and adjacent channels) results for RBF models and GaN HEMT Doherty.

In the second investigation, the accuracies of TLP and RBF models are compared for the case in which they are both trained by the GN algorithm. Different TLP and RBF models, having a variable number of neurons in the hidden layer and a variable memory length *M*, are implemented in Matlab software. Figure 13 shows the best ACEPR and NMSE results as a function of the number of network parameters. Differently from the two previously assessed DUTs, for the low-pass equivalent behavioral modeling of the GaN HEMT Doherty PA, TLP models provide a significant superior performance with respect to RBF models. Specifically, in case of identical number of parameters, TLP models achieve up to 8.4 dB and 8.7 dB improvements in NMSE and ACEPR results, respectively. Moreover, in case of comparable modeling accuracy, TLP requires a much lower set of network parameters. Indeed, a TLP model having 122 parameters can provide very confident estimations, attested by NMSE and ACEPR results of -42.4 dB and -50.3 dB, respectively.

Brazilian Microwave and Optoelectronics Society-SBMO *received 27 Feb 2015; for review 01 Mar 2015; accepted 19 Sep 2015*
Brazilian Society of Electromagnetism-SBMag *ISSN 2179-1074*

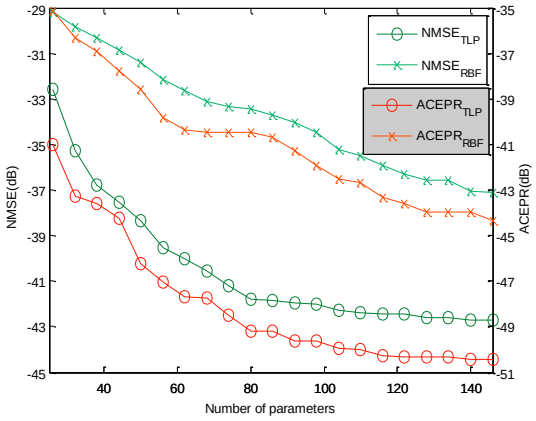

Fig. 13. NMSE and ACEPR (largest from lower and upper adjacent channels, bandwidth of 7.68 MHz for main and adjacent channels, frequency shift of 10 MHz between main and adjacent channels) results for GaN HEMT Doherty.

Figure 14 shows the normalized instantaneous amplitude of the PA output signal as a function of the instantaneous amplitude of the PA input signal, the so-called instantaneous AM-AM conversion. In this scenario of identical number of network parameters, it is observed that the TLP model clearly provides a better estimation than the RBF model.

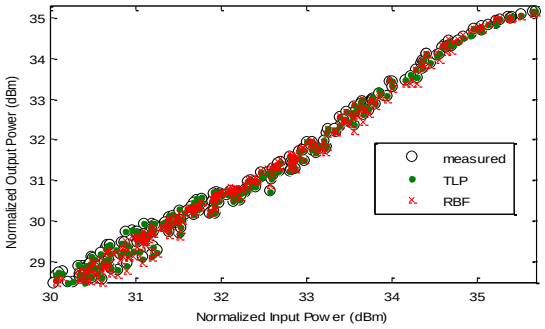

Fig. 14. Normalized instantaneous AM-AM conversion for TLP and RBF models having 68 network parameters, for modeling the GaN HEMT Doherty.

V. CONCLUSIONS

This work has presented a comparative analysis between TLP-based and RBF-based low-pass equivalent behavioral models for wireless transmitters. Input-output data obtained from three different DUTs were employed. Particular attention was paid to assess the TLP and RBF modeling accuracies (or, conversely, modeling errors) as a function of their number of parameters. The input signals applied to the TLP and RBF models were properly selected in order to simultaneously compensate for memory effects and guarantee the fulfillment of the constraints associated to the bandpass behavior of wireless transmitter under narrowband excitations. The reported results for the three investigated DUTs have shown that the choice of the training algorithm has a very significant impact on RBF models and that the commonly adopted OLS algorithm could not provide any accurate RBF model. In a scenario where all models were trained by the same nonlinear optimization tool based on the Gauss-Newton algorithm, the reported results have shown that, for two investigated DUTs, very similar performances were achieved by TLP and RBF models having the same number of network

  ISSN 2179-1074

parameters, with a somewhat superior performance for TLP models. Moreover, for one investigated DUT, a clearly superior performance was achieved by TLP models, in terms of modeling fidelity and computational burden, with respect to RBF models of same number of network parameters. Specifically, for an equal number of network parameters, TLP models have shown lower modeling errors than RBF models, quantified by: up to 0.5 dB and 1.5 dB improvements in NMSE and ACEPR results, respectively, when modeling the GaN HEMT class AB DUT; up to 0.7 dB and 1.2 dB improvements in NMSE and ACEPR results, respectively, when modeling the Si LDMOS class AB DUT; and up to 8.4 dB and 8.7 dB improvements in NMSE and ACEPR results, respectively, when modeling the GaN HEMT Doherty DUT.

ACKNOWLEDGMENT

The authors would like to thank the financial support provided by Coordenação de Aperfeiçoamento de Pessoal de Nível Superior (CAPES).

REFERENCES

[1] D. Raychaudhuri and N.B. Mandayam, "Frontiers of Wireless and Mobile Communications," *Proc. IEEE*, vol.100, no.4, pp.824-840, Apr. 2012.

[2] W. Chen, S. Zhang, Y.-J. Liu, F. M. Ghannouchi, Z. Feng, and Y. Liu, "Efficient Pruning Technique of Memory Polynomial Models Suitable for PA Behavioral Modeling and Digital Predistortion," *IEEE Trans. Microw. Theory Tech.*, vol.62, no.10, pp.2290–2299, Oct. 2014.

[3] G. Xu, T. Liu, Y. Ye, T. Xu, H. Wen, and X. Zhang, "Generalized Two-Box Cascaded Nonlinear Behavioral Model for Radio Frequency Power Amplifiers With Strong Memory Effects," *IEEE Trans. Microw. Theory Tech.*, vol.62, no.12, pp.2888–2899, Dec. 2014.

[4] H. Raab, P. Asbeck, S. Cripps, P. B. Kenington, Z. B. Popovic, N. Pothecary, J. F. Sevic, and N. O. Sokal, "Power amplifiers and transmitters for RF and microwave," *IEEE Trans. Microw. Theory Tech.*, vol.50, no.3, pp.814–826, Mar. 2002.

[5] S. Cripps, *RF Power Amplifiers for Wireless Communications*, 2nd edition. Norwood, MA: Artech House, 2006.

[6] P. B. Kenington, *High Linearity RF Amplifier Design*. Norwood, MA: Artech House, 2000.

[7] J. C. Pedro and S. A. Maas, "A comparative overview of microwave and wireless power-amplifier behavioral modeling approaches," *IEEE Trans. Microw. Theory Tech.*, vol. 53, no. 4, pp. 1150–1163, Apr. 2005.

[8] S. Haykin, *Neural Networks: a Comprehensive Foundation*, 2nd edition. New Jersey: Prentice Hall, 1999.

[9] T. Liu, S. Boumaiza, and F. M. Ghannouchi, "Dynamic behavioral modeling of 3G power amplifiers using real-valued time-delay neural networks," *IEEE Trans. Microw. Theory Tech.*, vol. 52, no. 3, pp. 1025–1033, Mar. 2004.

[10] E. G. Lima, T. R. Cunha, and J. C. Pedro, "A Physically Meaningful Neural Network Behavioral Model for Wireless Transmitters Exhibiting PM–AM/PM–PM Distortions", *IEEE Trans. Microw. Theory Tech.*, vol. 59, no. 12, pp. 3512–3521, Dec. 2011.

[11] X.-H. Yuan and Q. Feng, "Behavioral modeling of RF power amplifiers with memory effects using orthonormal Hermite polynomial basis neural network", *Prog. Electromagn. Res. C*, vol. 34, pp. 239–251, 2013.

[12] K. Fu, C. L. Law, and T. T. Thein, "Novel Neural Network Model of Power Amplifier Plus IQ Imbalances", *Prog. Electromagn. Res. B*, vol. 46, pp. 177–192, 2013.

[13] L. B. C. Freire, C. França, and E. G. Lima, "Low-pass equivalent behavioral modeling of RF power amplifiers using two independent real-valued feed-forward neural networks", *Prog. Electromagn. Res.C*, vol. 52, pp. 125–133, 2014.

[14] M. Isaksson, D. Wisell, and D. Ronnow, "Wide-band dynamic modeling of power amplifiers using radial-basis function neural networks," *IEEE Trans. Microw. Theory Tech.*, vol. 53, no. 11, pp. 3422–3428, Nov. 2005.

[15] M. Li, S. He, and X. Li, "Complex radial basis function networks trained by QR-decomposition recursive least square algorithms applied in behavioral modeling of nonlinear power amplifiers," *Int. J. RF Microw. C. E.*, vol. 19, no. 6, pp. 634–646, Nov. 2009.

[16] S. Chen, C. F. N. Cowan, and P. M. Grant, "Orthogonal least squares learning algorithm for radial basis function networks," *IEEE Trans. Neural Netw.*, vol. 2, no. 2, pp. 302–309, Mar. 1991.

[17] J. Dennis Jr., "Nonlinear least-squares," in *State of the Art in Numerical Analysis: Conference Proceedings*, D. A. H. Jacobs, Ed. London: Academic Press, 1977, pp. 269–312.

[18] M. S. Muha, C. J. Clark, A. Moulthrop, and C. P. Silva, "Validation of power amplifier nonlinear block models," in *IEEE MTT-S Int. Microwave Symp. Dig.*, Anaheim, CA, Jun. 1999, pp. 759–762.

[19] M. Isaksson, D. Wisell, and D. Ronnow, "A comparative analysis of behavioral models for RF power amplifiers," *IEEE Trans. Microw. Theory Tech.*, vol. 54, no. 1, pp. 348–359, Jan. 2006.

[20] A. V. Oppenheim and R. W. Schafer, *Discrete-time Signal Processing*, 3rd edition. Upper Saddle River, NJ: Pearson Higher Education, 2010.

received 27 Feb 2015; for review 01 Mar 2015; accepted 19 Sep 2015

ISSN 2179-1074